Density Functional Study on Regioselective Hydrolysis of a Tryptophan-Containing Peptide Promoted by Palladium(II) Complexes

Toshiaki Matsubara* and Kazuyuki Hirao

Institute for Fundamental Chemistry, 34-4 Takano-Nishihiraki-cho, Sakyo-ku, Kyoto 606-8103, Japan

Received June 11, 2001

The mechanism of hydrolysis of the model *N*-formyltryptophanamide (FmTrp-NH_2) with the $[Pd(en)]^{2+}$ (en = $H_2NC_2H_4NH_2$) complex has been theoretically examined by means of the density functional method (B3LYP). The calculations showed that the *N*-formyltryptophanamide easily binds to the $[Pd(en)]^{2+}$ complex to form the stereochemically stable six-membered ring in **2c**, where not only the carbonyl oxygen but also the indole carbon interact with the Pd atom. This interaction between the $[Pd(en)]^{2+}$ and the *N*-formyltryptophanamide is kept during the hydrolysis reaction to stabilize the energy surface and to reduce the energy barrier. On the other hand, the seven-membered ring formed by the coordination of the *C*-terminal amide oxygen to the Pd atom instead of the *N*-terminal amide oxygen was unfavorable in energy. The positive charge of the *N*-terminal amide carbon is remarkably enhanced by the formation of the Pd-binding *cis*-[Pd(en)*C*,*O*-FmTrp-NH_2)]$^{2+}$ **2c** and is selectively attacked by the negatively charged water oxygen, the electron being transferred from the water to the $[Pd(en)]^{2+}$ complex through the amide CO to promote the hydrolysis reaction. The positive charge of the water hydrogen remarkably increases in the transition state, so that the O−H bond is heterolytically broken and the H^+ migrates to the amide nitrogen. When the water attacks the *C*-terminal amide carbon in **2c**, such electron transfer is largely reduced and then the energy barrier increases. Thus, the regioselectivity experimentally observed was reasonably understood by the selective attack of water to the *N*-terminal amide carbon. It was also found that the stability of the potential energy surface and the energy barrier of the hydrolysis reaction can be controlled by the strength of the electron donation of the ligand of the Pd complex.

1. Introduction

It is widely known that metal complexes play an important role on the various biological processes.[1−3] In recent years, it has been experimentally reported that the palladium(II) complexes recognize the sequence of amino acids and selectively break the amide bond of peptides or proteins.[4,5] This is one of the greatly interesting subjects from the biochemical and molecular biological points of view, because the selective cleavage of peptides and proteins is an important procedure in those fields. The amide bond is extremely unreactive, and the reaction rate of hydrolysis is quite slow without the catalyst. Although chemical reagents such as cyanogen bromide requiring harsh reaction conditions or some enzymes that cleave the bond at many sites are known to promote the reaction,[5] the high selectivity in the cleavage is not expected at all. Therefore, an efficient catalyst for the selective cleavage has been strongly desired.

The highly regioselective hydrolysis of tryptophan-containing peptides with the $[Pd(en)]^{2+}$ (en = $H_2NC_2H_4$-NH_2) complex was recently experimentally reported by Kostić and co-workers.[6] The hydrolysis does not proceed without the palladium(II) complex. However, when equimolar amounts of a peptide and a palladium(II) complex are mixed in acetone solution at 50 °C with a stoichiometric amount of H_2O, the reaction is remarkably promoted and occurs selectively on the *N*-terminal side of the peptide, producing the *N*-terminal amino acid and the palladium(II) complex of *N*-acetyltryptophan, as shown in Scheme 1.

The breaking of the C−N bond of the *C*-terminal amide, which produces acetic acid, does not take place. The ^1H and ^{13}C NMR spectra have suggested that the *N*-acetyl-L-tryptophanamide (AcTrp-NH_2) binds to the $[Pd(en)]^{2+}$ complex to form the stereochemically stable

(1) (a) Cotton, F. A.; Wilkinson, G. In *Advanced Inorganic Chemistry*, 5th ed.; John Wiley & Sons: New York, 1988; Chapter 30, and references therein. (b) Crabtree, R. H. In *The Organometallic Chemistry of the Transition Metals*, 2nd ed.; John Wiley & Sons: New York, 1994; Chapter 16, and references therein.

(2) Alberts, B.; Bray, D.; Lewis, J.; Raff, M.; Roberts, K.; Watson, J. D. *Molecular Biology of the Cell*, 3rd ed.; Garland: New York, 1994.

(3) (a) Linder, M. C. *Biochemistry of Copper*; Plenum: New York, 1991. (b) Prasad, A. S. *Biochemistry of Zinc*; Plenum: New York, 1993. (c) Hausinger, R. P. *Biochemistry of Nickel*; Plenum: New York, 1993.

(4) (a) Parac, T. N.; Kostić, N. M. *J. Am. Chem. Soc.* **1996**, *118*, 51. (b) Parac, T. N.; Kostić, N. M. *J. Am. Chem. Soc.* **1996**, *118*, 5946. (c) Parac, T. N.; Ullmann, G. M.; Kostić, N. M. *J. Am. Chem. Soc.* **1999**, *121*, 3127.

(5) Croft, L. R. *Handbook of Protein Sequence Analysis*, 2nd ed.; Wiley: Chichester, 1980.

(6) Kaminskaia, N. V.; Johnson, T. W.; Kostic, N. M. *J. Am. Chem. Soc.* **1999**, *121*, 8663.

10.1021/om0105021 CCC: $20.00
Publication on Web 10/02/2001

Scheme 1

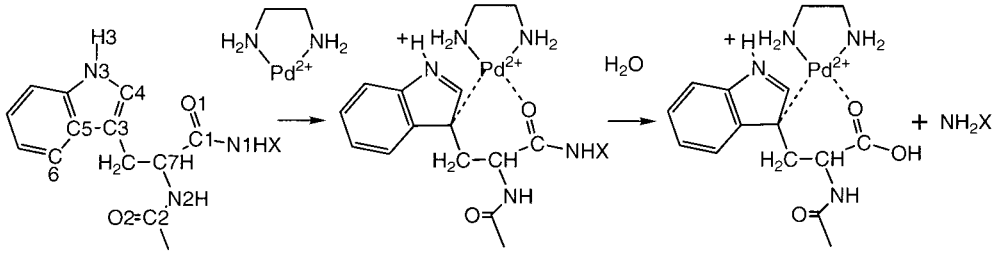

Table 1. Geometrical Parameters (in Å), *d*[C1(2)−N1(2)], *d*[N1(2)−H1], *d*[C1(2)−O3], and *d*[O3−H1], and the Mulliken Atomic Charges at the C1(2), N1(2), O1(2), O3, H1, and H2 Atoms of the Transition States TS1−2x (x = a−f)

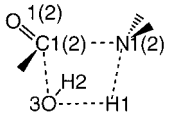

	d[C1(2)-N1(2)]	*d*[N1(2)-H1]	*d*[C1(2)-O3]	*d*[O3−H1]
free H_2O				0.977
free NH_3		1.009		
TS1a	1.554	1.183	1.928	1.333
TS1b	1.527	1.194	1.940	1.340
TS1c	1.513	1.303	1.748	1.235
TS1d	1.519	1.199	1.886	1.332
TS1e	1.504	1.223	1.892	1.316
TS1f	1.504	1.300	1.786	1.248
TS2a	1.565	1.212	1.889	1.307
TS2c	1.574	1.146	1.975	1.396
TS2f	1.610	1.306	1.713	1.212

	C1(2)	N1(2)	O1(2)	O3	H1	H2
free H_2O				−0.711	0.356	0.356
TS1a	0.120	−0.737	−0.260	−0.753	0.440	0.337
TS1b	0.175	−0.737	−0.345	−0.723	0.446	0.346
TS1c	0.277	−0.737	−0.346	−0.628	0.494	0.414
TS1d	0.387	−0.728	−0.330	−0.709	0.481	0.375
TS1e	0.313	−0.720	−0.341	−0.691	0.471	0.377
TS1f	0.295	−0.739	−0.307	−0.631	0.489	0.409
TS2a	0.051	−0.581	−0.346	−0.706	0.451	0.352
TS2c	0.084	−0.562	−0.282	−0.781	0.457	0.393
TS2f	0.136	−0.602	−0.300	−0.649	0.497	0.439

six-membered ring, where not only the carbonyl oxygen but also the indole carbon interact with the Pd atom (Scheme 1). On the other hand, the seven-membered ring formed by the coordination of the *C*-terminal amide oxygen to the Pd atom instead of the *N*-terminal amide oxygen was not observed. One will, therefore, consider that the *N*-terminal amide carbon whose positive charge would be enhanced by the formation of *cis*-[Pd(en)*C*,*O*-AcTrp-NHX)]$^{2+}$ becomes more susceptible to the nucleophilic attack of water compared with the *C*-terminal amide carbon.

In the present study, to clarify the promotion effect of the Pd complex and the origin of the regioselectivity, the details of the hydrolysis mechanism were theoretically investigated using the density functional method (B3LYP). *N*-Formyltryptophanamide as a peptide and [Pd(en)]$^{2+}$ as a palladium(II) complex were adopted. Since in the experiment the reaction rate of the hydrolysis is reduced to less than one-tenth when the [Pd(Me$_4$en)]$^{2+}$ (Me$_4$en = $Me_2NC_2H_4NMe_2$) complex is used instead of the [Pd(en)]$^{2+}$ complex, the effects of the ligand of the palladium(II) complexes were also examined using [Pd($H_2PC_2H_4PH_2$)]$^{2+}$ and the Pd^{2+} without ligand in addition to [Pd(en)]$^{2+}$ and [Pd(Me$_4$en)]$^{2+}$. Following the explanation of the computational methods in section 2, in section 3.1 hydrolysis without catalyst and with H_2O as a catalyst and in section 3.2 hydrolysis with the [Pd(en)]$^{2+}$ complex are discussed. In the subsequent sections, the origin of the regioselectivity and the ligand effects of the palladium(II) complex are discussed in sections 3.3 and 3.4, respectively, with the perspective of the molecular design for a more efficient reaction. Conclusions are given in the last section. The geometric parameters and the atomic charges for the equilibrium structures and the transition states are summarized in Tables 1 and 2. The potential energy surfaces of the hydrolysis reaction are presented in Figure 2 together.

2. Computational Methods

All the DFT calculations were performed using the Gaussian98 program.[7] The calculations of energies as well as geometry optimizations were carried out at the B3LYP level of theory, which consists of a hybrid Becke + Hartree−Fock exchange and Lee−Yang−Parr correlation functional with nonlocal corrections.[8] In the geometry optimizations, the basis set I, the lanl2dz[9,10] implemented by the Gaussian98 program, was used for all the atoms, H, C, N, O, P, and Pd.[11] All equilibrium structures and transition states were optimized without any symmetry restrictions and identified by the

Table 2. Important Geometrical Parameters (in Å) of 1−6x and TS1−2x (x = a−f)

	1	2x	TS1x	3x	4x	TS2x	5x	6x
x = a								
C1−O1	1.260	1.273	1.251	1.251	1.238			
C1−N1	1.367	1.355	1.554					
C1−C7	1.550	1.543	1.543	1.541	1.537			
C1−O3			1.978	1.348	1.384			
C2−O2	1.263	1.263				1.259	1.240	1.234
x = b								
C1−O1		1.276	1.268	1.316	1.238			
C1−N1		1.355	1.527	1.672				
C1−C7		1.545	1.542	1.566	1.536			
C1−O3			1.940	1.466	1.380			
x = c								
Pd−C3		2.262	2.271	2.269	2.264	2.259	2.292	2.262
Pd−C4		2.510	2.508	2.511	2.554	2.506	2.564	2.576
Pd−O1		2.073	2.074	2.039	2.101	2.071	2.083	2.078
Pd−O2		2.754	2.752	3.242	2.752	2.954		
C1−O1		1.286	1.303	1.366	1.264			
C1−N1		1.341	1.513	1.589				
C1−C7		1.545	1.549	1.564	1.535			
C1−O3			1.748	1.436	1.336			
C2−O2		1.258				1.245	1.249	1.234
x = d								
Pd−C3		2.435	2.720	2.408	2.446			
Pd−C4		2.536	2.318	2.498	2.558			
Pd−O1		2.100	2.103	2.073	2.100			
Pd−O2		4.023	4.113	4.989	4.047			
x = e								
Pd−C3		2.280	2.284	2.273	2.286			
Pd−C4		2.647	2.736	2.634	2.669			
Pd−O1		2.091	2.094	2.065	2.107			
Pd−O2		4.017	4.228	4.963	3.892			
x = f								
Pd−C3		2.071	2.211	2.128	2.067	2.076	2.211	2.123
Pd−C4		2.726	3.172	3.013	2.762	2.740	2.570	2.640
Pd−C5		2.667	2.321	2.388	2.672	2.874	3.017	2.631
Pd−C6		3.373	2.472	2.742	3.369	3.656	3.958	3.467
Pd−O1		2.107	2.053	2.034	2.208	2.197	2.021	2.060
Pd−O2		2.378	2.372	2.469	2.333	2.241	2.121	
C2−O2		1.259				1.278	1.255	1.234

number of imaginary frequencies calculated from the analytical Hessian matrix. The reaction coordinates were followed from the transition state to the reactant and the product using the intrinsic reaction coordinate (IRC) technique.[12]

For the optimized structures, single-point calculations were performed to obtain more reliable energies using the higher quality basis set II, including polarization functions, at the 6-31G** level[13,14] for all C, N, O, and P atoms and H of water and the *N*-terminal amide of *N*-formyltryptophanamide. For Pd, a triple-ζ (5s,5p,4d)/[3s,3p,3d] valence basis function augmented by a single set of f polarization functions with the exponent of 1.472[15] and the relativistic effective core potential (ECP) replacing the core electrons up to 3d determined by Hay and Wadt[16] were used. Although the energy calculations at the B3LYP/II level did not change the trend in the potential energy surface at the B3LYP/I level, the energy calculated at the B3LYP/II level is discussed unless otherwise indicated. The solvent effect was also calculated by the polarized-continuum-model (PCM) approximation[17] for the B3LYP/I-optimized geometries at the B3LYP/II level using acetone with the dielectric constant $\epsilon = 20.7$.

N-Formyltryptophanamide (FmTrp-NH_2), where the X and methyl substituents in the *N*- and *C*-terminal amide in *N*-acetyltryptophanamide are replaced by the H atom for convenience in the computations, was adopted as a peptide model. To examine the effects of the ligand of the palladium complex on the hydrolysis reaction, $[Pd(en)]^{2+}$, $[Pd(Me_4en)]^{2+}$, $[Pd(H_2PC_2H_4PH_2)]^{2+}$, and the bare Pd^{2+} atom without any ligand were used. The equilibrium structures and the transition states involved in the hydrolysis with the palladium(II) catalyst, $[Pd(en)]^{2+}$, $[Pd(Me_4en)]^{2+}$, $[Pd(H_2PC_2H_4PH_2)]^{2+}$, and Pd^{2+} are labeled by **c**, **d**, **e**, and **f**, and those in the hydrolysis without any catalyst and with H_2O as a catalyst are labeled by **a** and **b**, respectively.

3. Results and Discussion

3.1. Hydrolysis without the Palladium(II) Complex. Although the hydrolysis without the palladium(II) complex is extremely slow and virtually does not proceed in the experimental conditions as mentioned in the Introduction, we examined the system without the palladium(II) complex to compare with that with the palladium(II) complex and clarify the origin of the promotion effect of the palladium(II) complex in the following sections. Here, the reaction is restricted to only the hydrolysis on the *N*-terminal side, which has been experimentally observed in the system with the palladium(II) complex. The hydrolysis on the *C*-terminal side with and without the palladium(II) complex is discussed together in section 3.3.

The optimized equilibrium and the transition state structures involved in the hydrolysis without the catalyst (**1** → **4a**) are presented in Figure 1. In the reactant *N*-formyltryptophanamide **1**, the *N*-terminal and the *C*-terminal amides come close to each other to form the N1−H- - -O2 H-bonding with a distance of 1.884 Å. The incoming water first has an electrostatic interaction between the water oxygen and the hydrogen attached to the C7 in addition to the O−H- - -O1 H-bonding with a distance of 1.737 Å between the water O−H and the *N*-terminal amide oxygen in **2a**. The water migrates to the *N*-terminal amide side and the water OH bridges over the C1−N1 bond in the transition state **TS1a**, where the water oxygen and hydrogen are attached to the C1 and N1 atoms, respectively. After passing

(7) Frisch, M. J.; Trucks, G. W.; Schlegel, H. B.; Scuseria, G. E.; Robb, M. A.; Cheeseman, J. R.; Zakrzewski, V. G.; Montgomery, J. A., Jr.; Stratmann, R. E.; Burant, J. C.; Dapprich, S.; Millam, J. M.; Daniels, A. D.; Kudin, K. N.; Strain, M. C.; Farkas, O.; Tomasi, J.; Barone, V.; Cossi, M.; Cammi, R.; Mennucci, B.; Pomelli, C.; Adamo, C.; Clifford, S.; Ochterski, J.; Petersson, G. A.; Ayala, P. Y.; Cui, Q.; Morokuma, K.; Malick, D. K.; Rabuck, A. D.; Raghavachari, K.; Foresman, J. B.; Cioslowski, J.; Ortiz, J. V.; Stefanov, B. B.; Liu, G.; Liashenko, A.; Piskorz, P.; Komaromi, I.; Gomperts, R.; Martin, R. L.; Fox, D. J.; Keith, T.; Al-Laham, M. A.; Peng, C. Y.; Nanayakkara, A.; Gonzalez, C.; Challacombe, M.; Gill, P. M. W.; Johnson, B. G.; Chen, W.; Wong, M. W.; Andres, J. L.; Head-Gordon, M.; Replogle, E. S.; Pople, J. A. *Gaussian 98*; Gaussian, Inc.: Pittsburgh, PA, 1998.

(8) (a) Lee, C.; Yang, W.; Parr, R. G. *Phys. Rev. B* **1988**, *37*, 785. (b) Becke, D. *J. Chem. Phys.* **1993**, *98*, 5648.

(9) Dunning T. H., Jr.; Hay, P. J. In *Modern Theoretical Chemistry;* Schaefer, H. F., III, Ed.; Plenum: New York, 1976; Vol. 3, p 1.

(10) (a) Wadt, W. R.; Hay, P. J. *J. Chem. Phys.* **1985**, *82*, 284. (b) Hay, P. J.; Wadt, W. R. *J. Chem. Phys.* **1985**, *82*, 299.

(11) The tendencies found in the geometries optimized with basis set I without the polarization functions did not change even if the optimizations were performed with the polarization functions for the active part of the hydrolysis, indicating that basis set I is reliable enough.

(12) Fukui, K.; Kato S.; Fujimoto, H. *J. Am. Chem. Soc.* **1975**, *97*, 1.

(13) Hariharan, P. C.; Pople, J. A. *Chem. Phys. Lett.* **1972**, *66*, 217.

(14) Francl, M. M.; Pietro, W. J.; Hehre, W. J.; Binkley, J. S.; Gordon, M. S.; DeFrees, D. J.; Pople, J. A. *J. Chem. Phys.* **1982**, *77*, 3654.

(15) Ehlers, A. W.; Böhme, M.; Dapprich, S.; Gobbi, A.; Höllwarth, A.; Jonas, V.; Köhler, K. F.; Stegmann, R.; Veldkamp, A.; Frenking, G. *Chem. Phys. Lett.* **1993**, *208*, 111.

(16) Hay, P. J.; Wadt, W. R. *J. Chem. Phys.* **1985**, *82*, 299.

(17) (a) Cossi, M.; Barone, V.; Cammi, R.; Tomasi, J. *Chem. Phys. Lett.* **1996**, *255*, 327. (b) Fortunelli, A.; Tomasi, J. *Chem. Phys. Lett.* **1994**, *231*, 34. (c) Tomasi, J.; Persico, M. *Chem. Rev.* **1994**, *94*, 2027. (d) Floris, F.; Tomasi, J. *J. Comput. Chem.* **1989**, *10*, 616. (e) Pascual-Ahuir, J. L.; Silla, E.; Tomasi, J.; Bonaccorsi, R. J. *J. Comput. Chem.* **1987**, *8*, 778. (f) Mieritus, S.; Tomasi, J. *J. Chem. Phys.* **1982**, *65*, 239. (g) Mieritus, S.; Scrocco, E.; Tomasi, J. *J. Chem. Phys.* **1981**, *55*, 117.

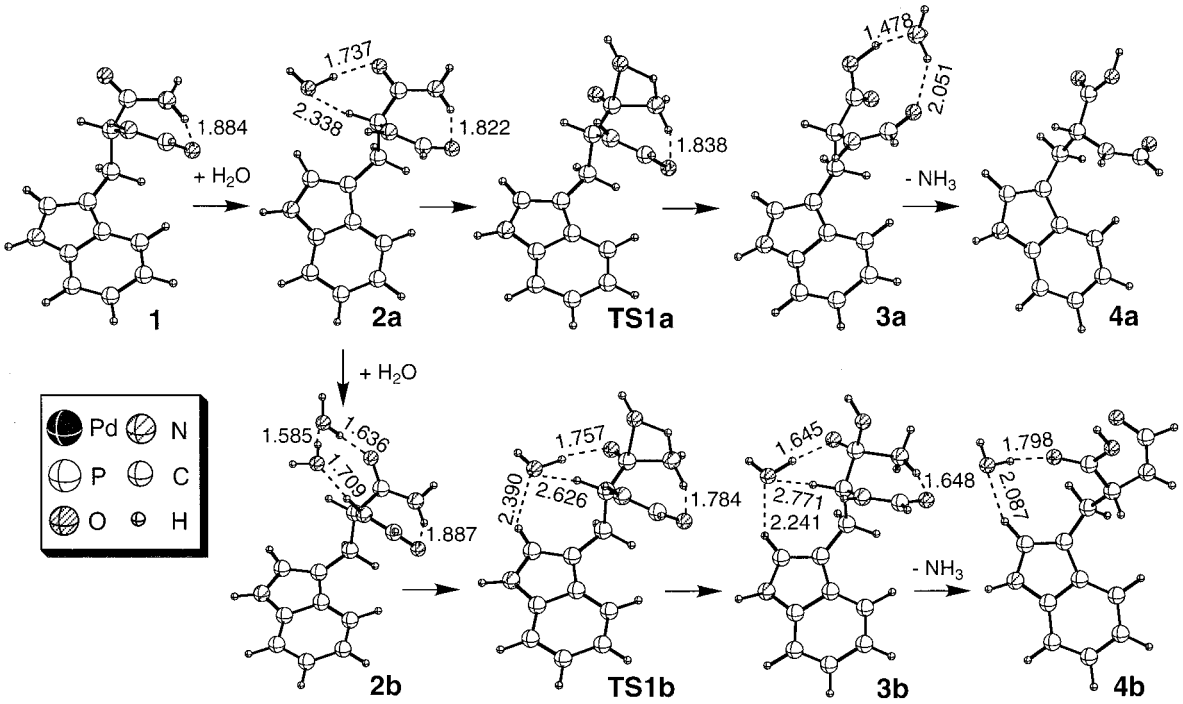

Figure 1. Optimized equilibrium and transition state structures at the B3LYP/I level for the hydrolysis of *N*-formyltryptophanamide by the attack of H_2O to the *N*-terminal amide with (from **1a** to **4b** through the transition state **TS1b**) and without H_2O as a catalyst (from **1** to **4a** through the transition state **TS1a**). The geometrical parameters (in Å) for the electrostatic interaction are presented. For the other geometrical parameters, see Tables 1 and 2.

through the transition state **TS1a**, the C1−N1 bond is broken to form *N*-formyltryptophan and NH_3. The decomposed NH_3 stays near the carboxyl substituent of the product, having the two H-bonds, O3−H2- - -N1 (1.478 Å) and N1−H- - -O2 (2.051 Å), in **3a**, and is completely away from *N*-formyltryptophan in **4a**.

As shown by the quite short N1−H1 distance of 1.183 Å and the long C1−O3 distance of 1.928 Å in **TS1a** (see Table 1), the electrophilic attack of the protonic water hydrogen to the negatively charged nucleophile N1 with the lone pair electron initiates the hydrolysis. The water hydrogen is abstracted as a proton by the nucleophile N1 in the first stage of the hydrolysis. In fact, in **TS1a**, although the C1−O3 distance is still kept long, the O3−H1 (1.333 Å) and the C1−N1 (1.554 Å) distances are already long and the N1 atom nearly has a tetrahedral structure. The electron is provided from the O1 to the N1 along the O1−C1−N1 linkage for the N1−H1 bonding, as presented below.

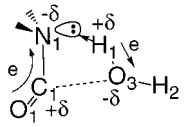

The Mulliken atomic charge decreases at the O1 from −0.302 e in **1** to −0.260 e in **TS1a**, while it increases at the N1 from −0.621 e in **1** to −0.737 e in **TS1a** as presented in Table 1. On the other hand, the electron in the H1−O3 is localized at the O3, as shown by the negative charge of −0.753 e, which is larger by −0.042 e than that of free water. The accumulated electron on the O3 is donated toward the C1 to form the C1−O3 bond in the second stage just after passing through **TS1a**. Therefore, the total charge of the H_2O (neutral) still remains unchanged in **TS1a**, although the H_2O molecule is more strongly polarized, in contrast to the case with the catalyst mentioned below. Thus, the O−H bond of the H_2O is heterolytically broken by the abstraction of H^+ by the nucleophile amide nitrogen.

Although the hydrolysis proceeds with a stoichiometric amount of H_2O in the experiment, the function of water as a catalyst was also examined. If we consider the water molecule as a catalyst in **2a**, another water molecule for the hydrolysis comes and at first breaks into the H−O- - -H(−C7) H-bond to form the multiple H-bond (N2−)H- - -O−H- - -O−H- - -O1 in **2b**. The water molecule migrates toward the *N*-terminal amide and bridges over the C1−N1 in the transition state **TS1b** in the same manner in the transition state **TS1a**. The slight rearrangement of the conformation of *N*-formyltryptophanamide causes the electrostatic interaction of the catalyst water oxygen with an indole hydrogen, which becomes stronger in **3b** and **4b** by its further conformational rearrangement, as shown by the shorter O- - -H distance of 2.241 Å in **3b** and 2.087 Å in **4b**, and shortens the O2- - -H−N1 H-bond between the *N*- and *C*-terminal amides to 1.784 Å.

The H-bond of water as a catalyst with the O1 atom in **2a** enhances a little the nucleophilicity of the C1 atom, because the positively charged water hydrogen stimulates the C1═O1 carbonyl oxygen to more polarize the carbonyl. In **TS1b**, the water coordinated to the O1 functions as an electron acceptor and slightly withdraws the electron from the O1−C1−N1 region, the total charge of the coordinated water becoming negative (−0.030 e). However, since the ability as an electron acceptor is quite low compared with the palladium(II) complex (see below), the geometrical structure of the transition state does not change so much as presented

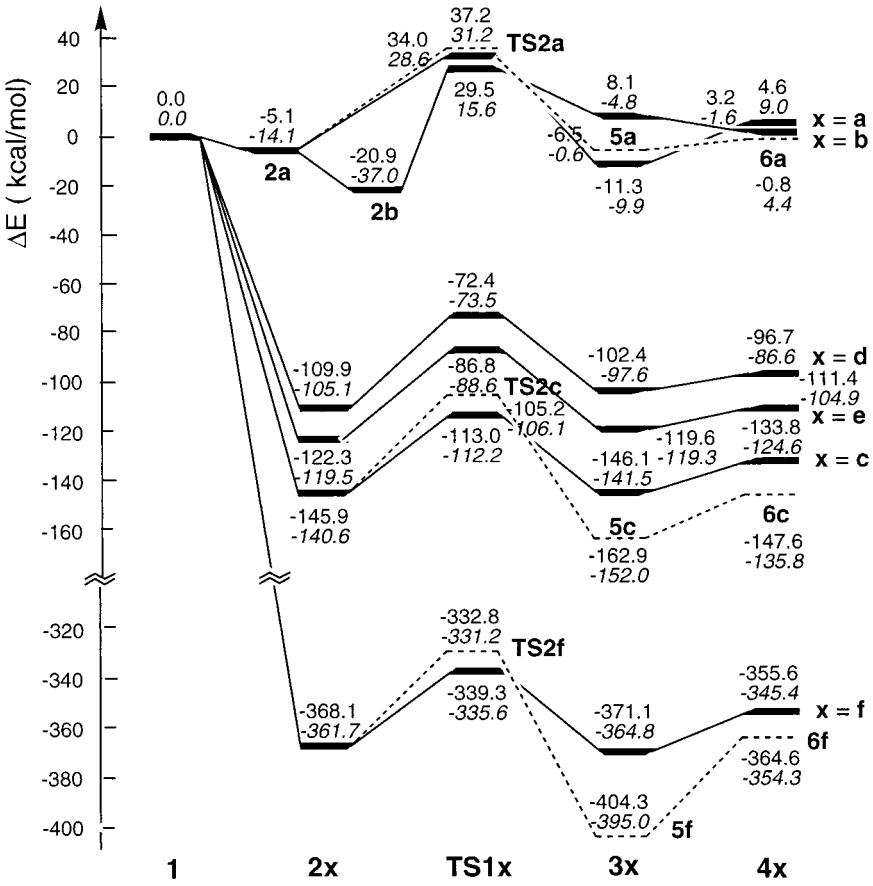

Figure 2. Potential energy surfaces (in kcal/mol) of the hydrolysis of *N*-formyltryptophanamide with the catalysts H_2O (**x** = **b**), $[Pd(en)]^{2+}$ (**x** = **c**), $[Pd(Me_4en)]^{2+}$ (**x** = **d**), $[Pd(H_2PC_2H_4PH_2)]^{2+}$ (**x** = **e**), and Pd^{2+} (**x** = **f**) and without the catalyst (**x** = **a**). The normal and dotted lines are for the hydrolysis by the attack of H_2O to the *N*-terminal and the *C*-terminal amide, respectively. The values in regular and italic type are calculated at the B3LYP/II and B3LYP/I levels, respectively.

in Table 1, indicating the same hydrolysis mechanism of the proton abstraction by the N1 atom. The coordinated water would thence somewhat thwart the proton abstraction because it reduces the nucleophilicity of the N1 atom due to the character of the electron acceptor.

In **3b** after the transition state **TS1b**, the formed NH_3 coordinates to the C1 atom without dissociation by the donation of its lone pair electron, which is different from the case in **3a**, because the C1 atom is affected by the electron acceptor water via the O1, becoming electron-deficient. The structural conformation of **4b** is different from that of **4a**, because the coordinated water by the H-bonding restricts the behavior of the carboxyl group in **4b**. Of course, although one can consider the participation of the water molecule more than as a catalyst, we did not treat such cases further. Even if we consider it, any significant effect of the water on the hydrolysis reaction will not be expected.

The potential energy surfaces of the hydrolysis without catalyst, **1** → **2a** → **TS1a** → **3a** → **4a**, and with water as a catalyst, **1** → **2a** → **2b** → **TS1b** → **3b** → **4b**, at the B3LYP/II level are presented in Figure 2. The hydrolysis without catalyst is 4.6 kcal/mol endothermic and the transition state **TS1a** is 34.0 kcal/mol higher in energy than the reactant **1**. *N*-Formyltryptophanamide is stabilized in energy by the coordination of water by 5.1 kcal/mol in **2a** and is further stabilized to form **2b** in the case of the hydrolysis with water as a catalyst. The electrostatic interaction of water as a catalyst shifts the potential energy surface down except for **3b** with the coordination of the formed NH_3. In **3b**, the coordinated water cannot stabilize enough the $O1^-$ anion formed by the sp^3-hybridization at the C1,[18] due to its weak electron acceptor in contrast to the case of the palladium(II) complex (see below). **4b** has an electrostatic interaction with the additional water. Nevertheless, it is only 1.4 kcal/mol more stable in energy than **4a**, because **4b** has structural stress which comes from the H-bonding with the water as mentioned above. Although the intermediates just before the transition states **TS1a** and **TS1b**, i.e., **2a** and **2b**, are stabilized by the electrostatic interaction with the incoming water as a substrate, the essential energy barrier for the hydrolytic cleavage of the amide should be evaluated separating the energy required for the breaking of the electrostatic interaction in **2a** and **2b** because the hydrolysis practically takes place after the complete breaking of the electrostatic interaction of the water as a substrate. That is, if we consider the energy difference between **1** and **TS1a** in the case without the catalyst water and between **2a** and **TS1b** in the case with water as a catalyst, the essential energy barrier for the hydrolysis is extracted. The energy barrier of 34.6 kcal/mol in the case with the additional water as a catalyst is, however, actually almost the same as that of 34.0 kcal/mol in the

(18) The C1−O1 and C1−C7 distances are stretched by the sp^3-hybridization at the C1 atom (see Table 2).

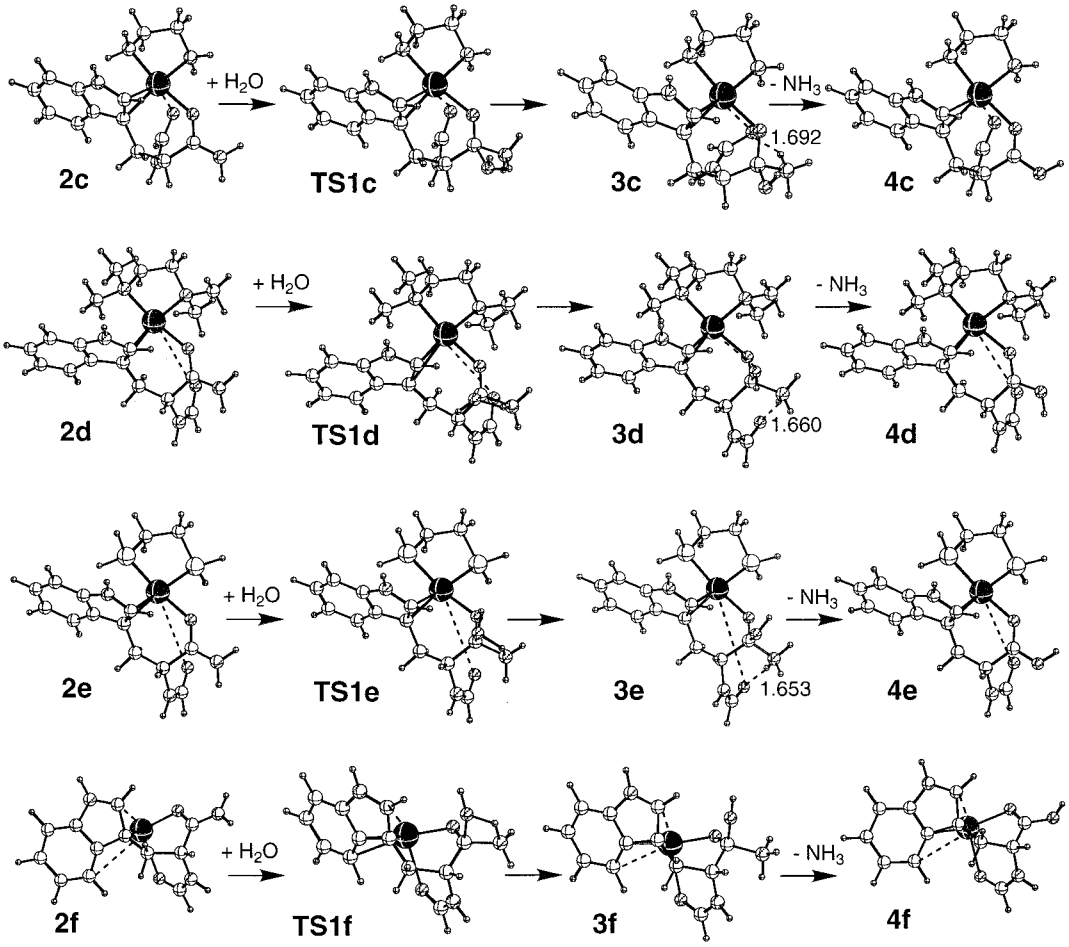

Figure 3. Optimized equilibrium and transition state structures at the B3LYP/I level for the hydrolysis of *N*-formyltryptophanamide by the attack of H_2O to the *N*-terminal amide with the catalysts $[Pd(en)]^{2+}$ (from **2c** to **4c** through the transition state **TS1c**), $[Pd(Me_4en)]^{2+}$ (from **2d** to **4d** through the transition state **TS1d**), $[Pd(H_2PC_2H_4PH_2)]^{2+}$ (from **2e** to **4e** through the transition state **TS1e**), and Pd^{2+} (from **2f** to **4f** through the transition state **TS1f**). Some geometrical parameters (in Å) for the electrostatic interaction are presented. For the other geometrical parameters, see Tables 1 and 2.

case without the catalyst water, indicating that the potential energy surface is slightly stabilized but the energy barrier is not changed by the consideration of water as a catalyst.

3.2. Hydrolysis with the $[Pd(en)]^{2+}$ Complex. As experimentally suggested,[6] the *N*-formyltryptophanamide easily binds to the palladium(II) complex, $[Pd(en)]^{2+}$, and forms the stable compound **2c** with the six-membered ring as presented in Figure 3. On the other hand, the seven-membered ring by the coordination of the *C*-terminal amide oxygen instead of the *N*-terminal amide oxygen to the Pd atom was stereochemically unfavorable and was not found as an equilibrium structure. The palladium(II) has the d^8 electron configuration so that the unoccupied d_{xy} orbital on the N−Pd−N plane (see Table 3) is provided for the interaction with *N*-formyltryptophanamide. Therefore, not only the *N*-terminal amide oxygen but also the indole carbon coordinate to the Pd atom by the donation of the lone pair electron to the unoccupied d_{xy} orbital of the Pd. As it is generally well known that the palladium(II) complex takes the four-coordinated square planar structure,[19] the $[Pd(en)]^{2+}$-bound compound by only the coordination of the O1 to the Pd was not found, which suggests that the interaction of the C3 with the Pd is necessary to form the stable compound. It is also obvious that two empty sites are demanded for the hydrolysis since the $[Pd(dien)]^{2+}$ (dien = $H_2NC_2H_4NHC_2H_4NH_2$)

Table 3. Mulliken Atomic Charge, Gross Orbital Population, and Molecular Orbital Energy (in Hartree) for the Pd of the Pd Complexes Pd^{2+} 1f, $[Pd(en)]^{2+}$ 1c, $[Pd(Me_4en)]^{2+}$ 1d, and $[Pd(H_2PC_2H_4PH_2)]^{2+}$ 1e

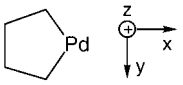

	1f	1c	1d	1e
		Mulliken Atomic Charge		
Pd	2.000	0.805	0.611	0.340
		Gross Orbital Population		
$4d_{xy}$	0.000	0.897	1.040	1.274
5s	0.022	0.290	0.301	0.368
$5p_z$	−0.002	0.012	0.035	0.010
$5s + 5p_z$	0.019	0.302	0.335	0.377
		Molecular Orbital Energy		
$4d_{xy}$	−0.994	−0.553	−0.481	−0.512
5s	−0.675	−0.427	−0.386	−0.393
$5p_z$	−0.469	−0.321	−0.282	−0.343

(19) Cotton, F. A.; Wilkinson, G. In *Advanced Inorganic Chemistry*, 5th ed.; John Wiley & Sons: New York, 1988; Chapter 19, and references therein.

complex, which provides only one site, exhibits no activity for the hydrolytic cleavage of the C−N amide bond.[6] By the coordination of the C3 to the Pd, a bond alternation occurs locally in the C3−C4−N3−H3 of the indole and the H3 is positively charged (see Scheme 1). The N3−C4 distance is shortened by 0.035 Å while the C4−C3 distance is elongated by 0.058 Å to switch the double and single bonds to each other. As a consequence, the electron is transmitted from the H3 to the C3 to produce the lone pair electron at the C3 atom. The positive charge of the H3 increased from 0.305 to 0.360 e and the N3−H3 distance was slightly stretched. However, in fact, the C4 also weakly coordinates to the Pd through its π orbital. We have theoretically found a similar type of cyclometalated complex as an intermediate in the aromatic C−H bond activation by the phosphine-coordinated Ru complex.[20] On the other hand, the O2 atom is also weakly bound to the Pd atom by the donation of the lone pair electron of the O2 to the unoccupied sp-hybridized orbital of the Pd perpendicular to the N−Pd−N plane. These interactions between the $[Pd(en)]^{2+}$ complex and the *N*-formyltryptophanamide are maintained during the reaction (**2c** → **4c**) to stabilize the energy surface of the reaction (see Table 2 for the geometrical parameters).

The positive charge of the *N*-terminal amide carbon C1 is remarkably enhanced from 0.208 to 0.422 e by the formation of the *cis*-[Pd(en)*C*,*O*-FmTrp-NH_2)]$^{2+}$ **2c**, because the electron in the C1═O1 region flows into the Pd by the electron donation from O1 to Pd. In contrast to the case without the palladium(II) complex (section 3.1), therefore, the water oxygen at first attacks the highly positively charged amide carbon C1 as presented below, as reflected in the geometrical parameters in the transition state **TS1c**, i.e., the short C1−O3 distance of 1.748 Å and the long N1−H1 distance of 1.303 Å.

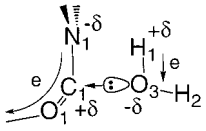

In the transition state **TS1c**, the electron is transmitted from the water to the strong electron acceptor $[Pd(en)]^{2+}$ complex having the unoccupied d orbital along the O3−C1−O1−Pd linkage. The negative charge of −0.628 e at the O3 is obviously smaller than that of −0.711 e for the free H_2O molecule (Table 1), and the total charge of the H_2O indicated the large positive charge of 0.280 e in **TS1c**. It should be noted that C1 is much more tetrahedral than N1 by the coordination of the H_2O oxygen to the C1 atom. The C1−O1 distance of 1.303 Å is stretched by 0.017 Å compared with that in **2c**, suggesting the incipient sp^3-hybridization at C1 and the formation of the $O1^-$ anion. The positive charge of the H_2O hydrogen remarkably increases to 0.494 e so that the H_2O hydrogen migrates to the N1 as a proton in the second stage of the hydrolytic cleavage. Therefore, both O3−H1 (1.235 Å) and C1−N1 (1.513 Å) distances are still short in **TS1c** compared with those in **TS1a**. Thus, the O−H bond of the H_2O is heterolytically broken on the C−N bond of the amide also in the case with the $[Pd(en)]^{2+}$ complex.

The formed NH_3 does not dissociate but coordinates to the C1 atom in **3c** with a distance of 1.589 Å, where one of the NH_3 hydrogens has an N1−H- - -O2 H-bond, because the strong electron acceptor $[Pd(en)]^{2+}$ makes the donation of the lone pair electron of the N atom to the C1 atom facile. The fact that the C1−N1 distance is shorter in **3c** (1.589 Å) than in **3b** (1.672 Å) is in accordance with the order in the strength of the electron acceptor, $[Pd(en)]^{2+} > H_2O$. The strong electron donation of the $O1^-$ anion to the Pd, which is reflected in the short Pd−O1 distance of 2.039 Å, weakens the donation of the lone pair electron of the O2 to the Pd, as shown by the Pd−O2 distance, which is stretched to 3.242 Å in **3c**. The sp^3-hybridization at the C1 atom also affects the C1−C7 bond distance and elongates it to 1.564 Å. By the dissociation of the electron donor NH_3, the Pd−O2 distance is again shortened in **4c**. On the other hand, the Pd−O1 distance becomes largest (2.101 Å), since the strong elecrophilicity of the OH substituent attached to the C1 atom reduces the electron donation of the O1 to the Pd.

As presented in Figure 2, the entire potential energy surface from **2c** to **4c** is largely shifted down compared with that without the palladium(II) complex, because both the equilibrium and the transition state structures are stabilized by the strong binding of the $[Pd(en)]^{2+}$ complex throughout the reaction. The energy barrier of 32.9 kcal/mol was smaller than that for the hydrolysis without the palladium(II) complex by the electronic effect of the $[Pd(en)]^{2+}$ complex, although the tight binding of the Pd during the reaction would restrict the conformational rearrangement of the peptide. This indicates that in the two different types of hydrolytic cleavage with and without the palladium(II) complex, i.e., (i) the H_2O oxygen coordination and then the H^+ migration, and (ii) the H^+ abstraction and then the OH^- migration, the former is easier than the latter. The step of the dissociation of the produced NH_3 (**3** → **4**) is 12.3 kcal/mol endothermic, although it is 4.9 kcal/mol exothermic in the reaction system with an additional water as a catalyst, because the strong electron acceptor $[Pd(en)]^{2+}$ enhances the NH_3 coordination and stabilizes the intermediate **3c** in energy as mentioned above. The remarkable promotion of the hydrolysis by the $[Pd(en)]^{2+}$ complex observed experimentally is, thus, reasonably understood, since the entire potential energy surface is stabilized and the highest point at the transition state **TS1c** is lowered by the electronic effect of the coordinated $[Pd(en)]^{2+}$ complex. In the sense that the $[Pd(en)]^{2+}$ complex activates the reaction field through its binding, the function of the $[Pd(en)]^{2+}$ complex as catalyst would be quite unique. One will here immediately notice that the reaction can be controlled by the electronic nature of the ligand of the $[Pd(en)]^{2+}$ complex, which is discussed in section 3.4.

3.3. Origin of the Regioselectivity. If the incoming H_2O attacks not the *N*-terminal side but the *C*-terminal side, the *C*-terminal amide is hydrolyzed to form formic acid. However, the hydrolytic cleavage indeed proceeds on the *N*-terminal side regioselectively in the experiment. Therefore, to examine the origin of the regioselectivity of the hydrolysis, calculations were also per-

(20) (a) Matsubara, T.; Koga, N.; Musaev, D. G.; Morokuma, K. *J. Am. Chem. Soc.* **1998**, *120*, 12692. (b) Matsubara, T.; Koga, N.; Musaev, D. G.; Morokuma, K. *Organometallics* **2000**, *19*, 2318.

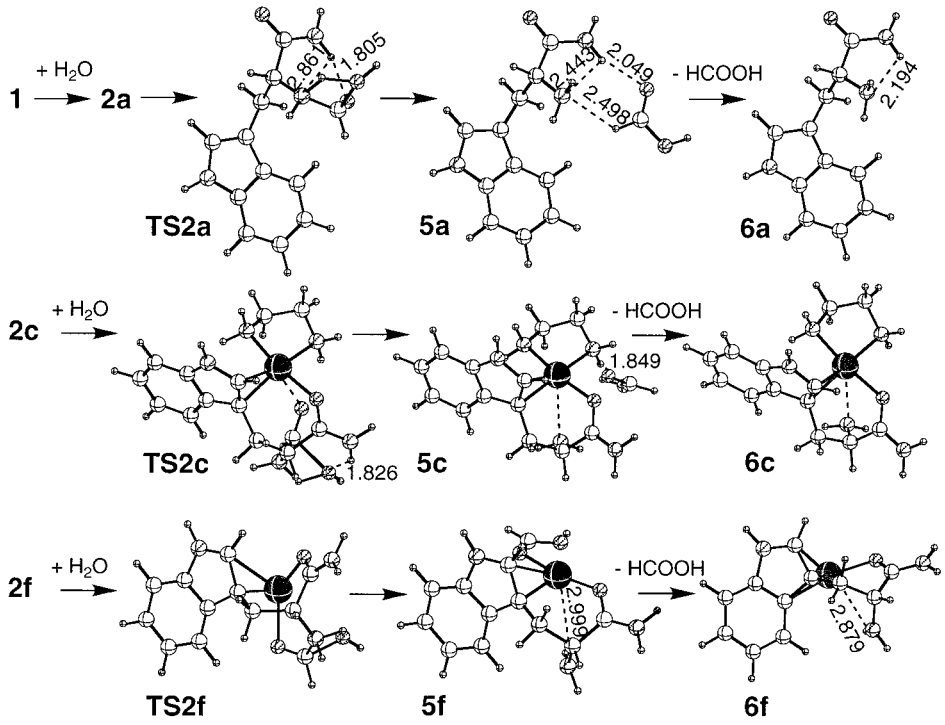

Figure 4. Optimized equilibrium and transition state structures at the B3LYP/I level for the hydrolysis of *N*-formyltryptophanamide by the attack of H_2O to the *C*-terminal amide with the catalysts $[Pd(en)]^{2+}$ (from **2c** to **6c** through the transition state **TS2c**) and Pd^{2+} (from **2f** to **6f** through the transition state **TS2f**) and without the catalyst (from **1** to **6a** through the transition state **TS2a**). The geometrical parameters (in Å) for the electrostatic interaction are presented. For the other geometrical parameters, see Tables 1 and 2.

formed for the reaction on the *C*-terminal side with and without the $[Pd(en)]^{2+}$ complex.

As presented in Figure 4, in the system without $[Pd(en)]^{2+}$ complex, starting from **1** the reaction forms the intermediate **2a** before the transition state **TS2a**, which is common in the case of hydrolysis on the *N*-terminal side. After passing through the transition state **TS2a**, the hydrolytic cleavage produces formic acid in **5a**, where the produced formic acid binds to the tryptophanamide by both O−H and N−H electrostatic interaction. The N2−H- - -N1 H-bond is shortened to 2.194 Å in **6a** by the dissociation of formic acid. Table 1 shows that the geometrical features of the transition state **TS2a** are nearly the same as those of the transition state **TS1a** for the hydrolysis on the *N*-terminal side. The characteristic in the mechanism of the OH^- migration to the C2 after the H^+ abstraction by N2 rather than H^+ migration to N2 after the H_2O oxygen coordination to the C2 is evidently reflected in the geometrical parameters of the long C2−O3 and C2−N2 distances and the short N2−H1 distance in **TS2a**.

In the system with the $[Pd(en)]^{2+}$ complex, although it is expected that the hydrolysis on the *C*-terminal side would also be enhanced by the formation of the seven-membered ring with the coordination of the *C*-terminal amide oxygen instead of the *N*-terminal amide oxygen to the Pd atom, the seven-membered ring was unfavorable in energy and is not formed as mentioned above. The reaction, therefore, starts from **2c** by the attack of H_2O to the *C*-terminal amide. In **2c**, since the interaction of the O2 with the Pd by the donation of the lone pair electron to the sp-hybridized orbital of the Pd perpendicular to the N−Pd−N plane is very weak as shown by the long Pd−O2 distance of 2.754 Å, the nature of the strong electron acceptor of the Pd is little available on the *C*-terminal side. In fact, in **TS2c**, the total charge of the H_2O shows the small positive charge of only 0.069 e, indicating that the donation of the lone pair electron of the H_2O oxygen to the C2 is quite small. As shown by the long C2−O3 distance of 1.975 Å and the short N2−H1 distance of 1.146 Å in **TS2c**, the reaction takes the mechanism of H^+ abstraction followed by OH^- migration to liberate formic acid. The change in the character of the bonding C2−N2 from covalent to coordination results in the long C2−N2 distance of 1.574 Å in **TS2c**. As shown by the large negative charge of the H_2O oxygen (−0.781 e), the O−H bond is strongly polarized and the electron is accumulated on the O3 for OH^- migration to the positively charged C2 in the second stage of the reaction. In **TS2c**, no elongation was found in the C2−O2 bond as presented in Table 2, because the sp^3-hybridization at C2 is not needed without the interaction of the H_2O oxygen with C2. In both **5c** and **6c** after hydrolytic cleavage, N2 instead of O2 interacts with the Pd atom by the donation of a lone pair electron of the N2 to the Pd atom.

The potential energy surface of the hydrolysis on the *C*-terminal side without the $[Pd(en)]^{2+}$ complex is only slightly shifted up, except for **6a**, compared to the corresponding potential energy surface of the hydrolysis on the *N*-terminal side as presented in Figure 2. Since the O2- - -H−N1 H-bond is kept during the hydrolysis reaction, the positively charged hydrogen attached to the O2 might slightly prevent the electron transmission from the O2 to the N2 along the O2−C2−N2 linkage to decrease the nucleophilicity of the N2 (see section 3.1). The computational result that **TS2a** is less stable by

3.2 kcal/mol than **TS1a** would be ascribed to this effect of the O2- - -H−N1 H-bond.

When the $[Pd(en)]^{2+}$ complex is added to the system, the potential energy surface is largely stabilized by the binding of the $[Pd(en)]^{2+}$ complex to the peptide as mentioned above. However, **TS2c** is 8.2 kcal/mol higher in energy than **TS1c**. This energy difference comes from the hydrolysis mechanism on the *C*-terminal side different from that on the *N*-terminal side aforementioned. When H_2O attacks the *C*-terminal amide in **2c**, the electron flow from the H_2O to the Pd for the energetically favorable mechanism initiated by the coordination of the H_2O oxygen to the C2 is shut off, because the O2−Pd interaction is too weak to transmit the electron through the O3−C2−O2−Pd linkage. Instead, the electron flow from O2 to N2 along the O2−C2−N2 linkage for the energetically less favorable mechanism of H^+ abstraction by N2 followed by OH^- migration to C2 is enhanced. Thus, the regioselective hydrolysis on the *N*-terminal side experimentally observed is reasonably explained by the selective attack of H_2O to the *N*-terminal amide induced by the electronic effect of the $[Pd(en)]^{2+}$ complex.

3.4. Effects of the Ligand. As mentioned in sections 3.2 and 3.3, the high reactivity and regioselectivity of the hydrolysis with the $[Pd(en)]^{2+}$ complex originate from the character of the electron acceptor of the $[Pd(en)]^{2+}$ complex. Therefore, the reaction would be controlled by the modification of the ligand which strongly affects the character of the electron acceptor of the palladium complex. From the viewpoint of the molecular design of more efficient hydrolysis catalysts, the effects of the ligand on the hydrolysis reaction were examined using the palladium(II) complexes other than $[Pd(en)]^{2+}$, $[Pd(Me_4en)]^{2+}$, $[Pd(H_2PC_2H_4PH_2)]^{2+}$, and Pd^{2+} without ligand.

Some important parameters for the unoccupied orbitals, $4d_{xy}$ in the plane of the chelate ligand and 5s and $5p_z$ perpendicular to the plane of the chelate ligand, which well express the strength of the electron acceptor of the palladium(II) complexes, are presented in Table 3. The atomic charge of +2 of the Pd^{2+} without ligand decreases when the ligand is attached because the electron is donated from the ligand to the Pd atom. The order in the atomic charge, **1c** > **1d** > **1e**, reflects the strength of the donation of the lone pair electron on N or P of the ligand to the $4d_{xy}$ orbital of the Pd atom; when the H attached to the N atom of the $H_2NC_2H_4NH_2$ ligand is replaced by the more electron donative Me substituent, the positive charge of the Pd atom decreases. When the N atom is replaced by the P atom, the sequence in the electronegativity being N(3.04) > P(2.19),[21] the positive charge of the Pd atom further decreases. Therefore, the gross orbital population of $5s+5p_z$ as well as $4d_{xy}$ increases in the order **1e** > **1d** > **1c** > **1f**, and the molecular orbital energy of $4d_{xy}$ and $5s+5p_z$ is stabilized in the order **1f** > **1c** > **1e** > **1d**. Thus, the strength of the character of the Pd atom as the electron acceptor is changed by the ligand. Here, one will easily predict that with the decrease in the electron acceptor character of the Pd, the binding of the Pd is weakened (the potential energy surface is destabilized) and the electron donation of the H_2O oxygen to the C1 atom in the transition state is depressed to make the hydrolysis more difficult.

The equilibrium and the transition state structures involved in the hydrolysis with the palladium(II) catalysts, $[Pd(Me_4en)]^{2+}$ **1d**, $[Pd(H_2PC_2H_4PH_2)]^{2+}$ **1e**, and Pd^{2+} **1f**, are presented together in Figure 3. The bonding of the O1 and the C3 to the Pd by donation of the lone pair electron to the $4d_{xy}$ orbital of the Pd atom is influenced by the strength of the electron donation of the ligand as expected. The Pd−O1 and Pd−C3 distances in **2d** and **2e** become longer than those in **2c**, while the Pd−C3 distance in **2f** becomes shorter (see Table 2). The Pd−O1 distance in **2f** is longer than that in **2c**, because O1 shares the interaction with the Pd atom with O2 competing in the electron donation to the Pd. The sequence in the Pd−O1 and the Pd−C3 distances, **2d** > **2e**, seems to be reversed according to the electronic effect of the ligand. However, it should be reasonable if the steric effect of the ligand is taken into account. That is to say, the large steric repulsion between the Me substituents and the peptide might weaken the Pd binding. This influences not only the stabilization of the potential energy surface but also the energy barrier, which is closely related to the electron transmission from the peptide to the Pd (see below). The weak Pd−O2 interaction by the donation of the lone pair electron of O2 to Pd is broken and the O2 atom is completely away from the Pd atom during the reaction in the case of $[Pd(Me_4en)]^{2+}$ and $[Pd(H_2PC_2H_4PH_2)]^{2+}$, which differs from the case of $[Pd(en)]^{2+}$, due to the strong electron donation of the ligand to Pd, which reduces the character of the electron acceptor of Pd. However, in both **3d** and **3e**, the produced NH_3 coordinates to C1 without dissociation by the donation of the lone pair electron of the NH_3 to the C1 connecting to Pd via O1.

We can find some tendencies in the geometrical parameters and the atomic charges in the transition state collected in Table 1. The C1−O3 and O3−H1 distances become longer in the order **TS1e** ≥ **TS1d** > **TS1f** > **TS1c** and **TS1d** > **TS1e** > **TS1f** > **TS1c**, respectively, while the N1−H1 distance becomes shorter in the order **TS1c** ≥ **TS1f** > **TS1e** ≥ **TS1d**. This suggests the shift of the mechanism from (i) H_2O oxygen coordination followed by H^+ migration to (ii) H^+ abstraction followed by OH^- migration. Indeed, electron donation from the H_2O oxygen to the C1 in the transition state, which causes an electron flow from the H_2O to the unoccupied d orbital of the Pd along the O3−C1−O1−Pd linkage, is suppressed by the ligand which is more electron donative. The positive charge of the H_2O decreases in the order **TS1c** > **TS1f** > **TS1e** > **TS1d**, indicating the scale of the electron flow with the same order. It is not surprising that the electron flow is not the largest in **TS1f**, because the bare Pd^{2+} is not so electron-deficient due to the strong electron donation from both O1 and O2 to the Pd. The sequence in the electron flow, **TS1c** > **TS1f** > **TS1e** > **TS1d**, apparently appears in the tendencies in the atomic charges; the negative charge at the O3 and the positive charge at the C1 decrease in the order **TS1d** > **TS1e** > **TS1f** > **TS1c**, while the positive charge at the H1 increases in the reverse order.

To make more clear the relationship between the

(21) Pauling's values are presented. For example, see: *The Elements*, 2nd ed.; Emsley, J., Ed.; Oxford University Press: New York, 1991.

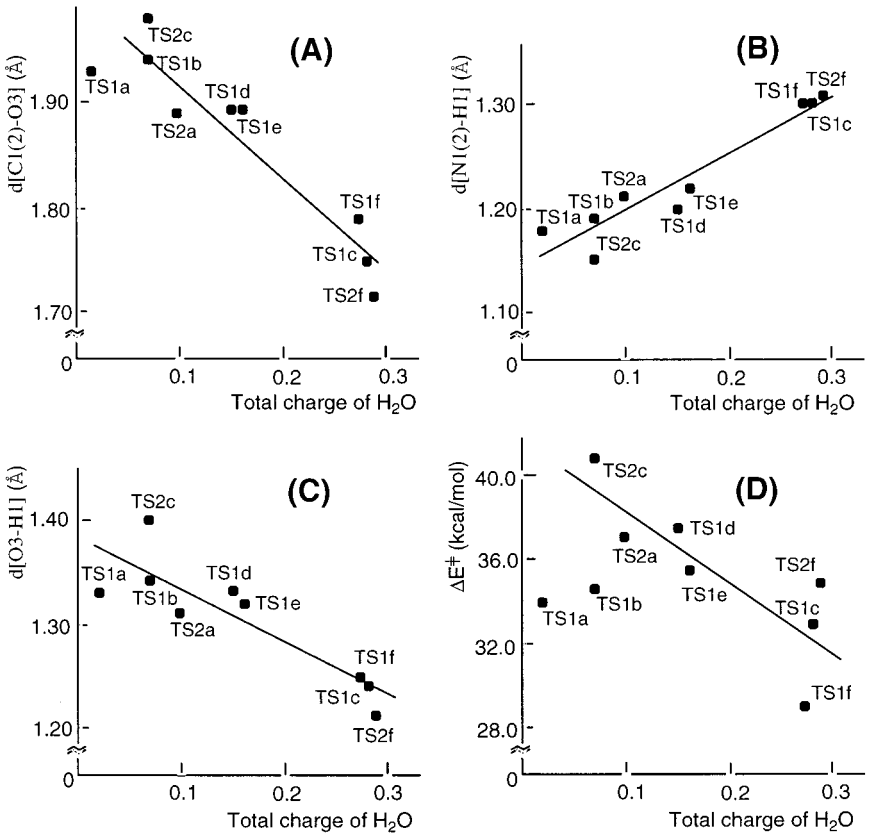

Figure 5. Plots of the distances (Å), *d*[C1(2)−O3] (A), *d*[N1(2)−H1] (B), and *d*[O3−H1] (C) in the transition states **TS1**−**2x** (**x** = **a**−**f**), and the energy barrier $\Delta E^{\ddagger}$ (kcal/mol) (D) versus the total charge of H_2O. The energy barrier is $\Delta E^{\ddagger}$(**1**→**TS1a**) for TS1a without the catalyst, $\Delta E^{\ddagger}$(**2a**→**TS1b**) for TS1b with the H_2O as a catalyst and $\Delta E^{\ddagger}$(**2x**→**TS1**−**2x**) for TS1−2x (x = c−f) with the Pd catalysts.

strength of the electron donation from the H_2O to the C1 and the geometric parameters of the transition state, the distances *d*[C1(2)−O3], *d*[N1(2)−H1], and *d*[O3−H1] of the transition states **TS1** and **TS2** were plotted, respectively, versus the total charge of the H_2O. As shown in A, B, and C in Figure 5, a linear relationship was obtained in each plot; the C1(2)−O3 and O3−H1 distances become longer, while the N1(2)−H1 distance becomes shorter with the decrease in the electron donation from the H_2O oxygen to the C1. This obviously indicates that the transition state shifts from **I** to **II** as illustrated below with the decrease in the electron donation from the H_2O oxygen to the C1.

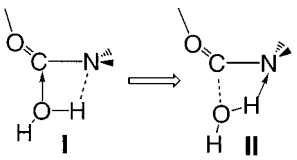

The typical two transition states, type **I** and **II**, are **TS1c** and **TS1a**, respectively, which reflects the two different hydrolysis mechanisms as mentioned above: (i) H_2O oxygen coordination to the C1 followed by H^+ migration to the N1, and (ii) H^+ abstraction by the N1 followed by OH^- migration to the C1.

The entire potential energy surface of the hydrolysis reaction was stabilized in the order Pd^{2+} > $[Pd(en)]^{2+}$ > $[Pd(H_2PC_2H_4PH_2)]^{2+}$ > $[Pd(Me_4en)]^{2+}$, according to the binding energy between the Pd and the peptide, as presented in Figure 2. One will also notice that the energy required for the NH_3 dissociation (**4** → **5**) has consistently the same order. On the other hand, the energy barrier decreases with the stabilization of the potential energy surface. These results are in agreement with the experimental finding[6] that the reaction rate is smaller for $[Pd(Me_4en)]^{2+}$ than for $[Pd(en)]^{2+}$.

The plot of the energy barrier against the total charge of the H_2O (Figure 5D) also gave a good correlation between them. The energy barrier decreases with the increase in the donation from the H_2O oxygen to the amide carbon. Since in the case of Pd^{2+} the distance of the Pd−O2 is also short, suggesting that the electron donation from O2 to Pd is relatively easy, it is predicted that the energy barrier would be small even for hydrolysis on the *C*-terminal amide. The optimized equilibrium and the transition state structures and the potential energy surface for the hydrolysis with the Pd^{2+} on the *C*-terminal side are presented in Figures 4 and 2, respectively. As expected, the structure of the transition state was type **I** rather than type **II** presented above due to the strong electron donation of the H_2O oxygen to the *C*-terminal amide carbon, and the energy barrier was 35.3 kcal/mol, as presented as the point TS2f in the plots in Figure 5. Without the rigid binding of the Pd, the conformation of the peptide can be relaxed to stabilize the transition state and to reduce the energy barrier. In fact, without the Pd catalyst the conformation of the peptide gradually changes as the hydrolysis reaction proceeds, as presented in Figure 1. Therefore,

Table 4. Potential Energies (in kcal/mol) for 2−6x and TS1−2x (x = a−f) Relative to 1 at the PCM-B3LYP/II Level in Acetone with the Dielectric Constant $\epsilon = 20.7$

	2x	TS1x	3x	4x	ΔE(R→TS1x)[a]
x = a	−1.1	37.6	−8.6	5.0	37.6 (34.0)
b	−13.5	35.9	10.3	6.5	37.0 (34.6)
c	−76.9	−40.6	−73.9	−64.7	36.3 (32.9)
d	−69.1	−27.8	−58.6	−55.3	41.3 (37.5)
e	−77.4	−37.4	−69.3	−65.2	40.0 (35.5)
f	−225.6	−194.2	−225.2	−212.3	31.4 (28.8)

	TS2x	5x	6x	ΔE(R→TS2x)[a]
x = a	39.5	−4.2	0.7	39.5 (37.2)
c	−30.0	−85.3	−80.0	46.9 (40.7)
f	−188.4	−254.1	−224.2	37.2 (35.3)

[a] **R** is **1** for **x** = **a**, **2a** for **x** = **b**, and **2x** for **x** = **c**−**f**. The numbers in parentheses are for the gas phase.

the points TS1a and TS1b for the case without the Pd complex deviate from the linearity in plot D.

The PCM calculations were performed at the B3LYP/II level for the B3LYP/I-optimized geometries to take the solvent effect into account using acetone with a dielectric constant $\epsilon = 20.7$, because the hydrolysis proceeds in acetone in experiment. The results are summarized in Table 4. The potential energy surfaces are destabilized by the effect of the solvation, which is notable especially for the reaction system with the palladium(II) complex. However, the tendency in the energy barrier is not changed, although the energy barrier becomes a few kcal/mol larger.

The results presented in this section certainly suggest that the reactivity can be controlled by the electronic effect of the ligand, and the less electron donative ligand more efficiently functions as a catalyst for the hydrolytic cleavage because it stabilizes the potential energy surface of the reaction and lowers the highest point at the transition state by the stronger binding of the Pd to the peptide and simultaneously promotes the electron donation from the H_2O oxygen to the amide carbon to reduce the energy barrier.

4. Concluding Remarks

The origin of the regioselectivity and the promotion effect of the palladium(II) complex $[Pd(en)]^{2+}$ on the hydrolysis of a tryptophan-containing peptide was theoretically examined by means of the density functional method (B3LYP) using the model peptide *N*-formyltryptophanamide. The calculations showed that the *N*-formyltryptophanamide easily binds to the $[Pd(en)]^{2+}$ complex to form the stereochemically stable compound **2c** with the six-membered ring, where not only the carbonyl oxygen but also the indole carbon interact with the Pd atom, and its binding is kept during the hydrolysis reaction to stabilize the energy surface and reduce the energy barrier. The positive charge of the *N*-terminal amide carbon is remarkably enhanced by the formation of *cis*-$[Pd(en)C,O\text{-FmTrp-NH}_2)]^{2+}$ **2c**, and thereby, the water oxygen selectively attacks the *N*-terminal amide carbon and the electron is transferred from the water to the electron acceptor $[Pd(en)]^{2+}$ complex along the O3(water)−C1−O1−Pd linkage. The largely positively charged water hydrogen migrates as a proton to the amide nitrogen to break the C−N bond of the amide. The good correlation found between the energy barrier and the strength of the electron donation of the ligand suggested that the ligand plays a key role in the reaction, and the less electron donative ligand is more efficient for the hydrolysis from the viewpoint of the molecular design of the catalyst.

Acknowledgment. Part of the calculations were carried out at the Computer Center of the Institute for Molecular Science, Japan. T.M. was partly supported by the Grants-in-Aid from the Ministry of Education, Science, Sports, and Culture, Japan.

Supporting Information Available: Listings giving the optimized Cartesian coordinates of all equilibrium structures and transition states presented in this paper. This material is available free of charge via the Internet at http://pubs.acs.org.

OM0105021